

PNAS

www.pnas.org

Supplementary Information for

Why Wild Giant Pandas Frequently Roll in Horse Manure

Wenliang Zhou^{1#}, Shilong Yang^{2,3#}, Bowen Li^{2#}, Yonggang Nie^{1,4#}, Anna Luo^{2,5}, Guangping Huang¹, Xuefeng Liu⁶, Ren Lai^{2*}, Fuwen Wei^{1,4,5*}

Corresponding author: Fuwen Wei and Ren Lai
Email: weifw@ioz.ac.cn, rlai@mail.kiz.ac.cn

This PDF file includes:

Supplementary text
Figures S1 to S3
Tables S1 to S3
Legends for Movies S1 to S4
SI References

Other supplementary materials for this manuscript include the following:

Movies S1 to S4

Supplementary Information Text

Materials and Methods

Study area of filed observation

Foping National Nature Reserve (FNNR) (E: 107°40'-107°55', N: 33°32'-33°45') is situated in the Qinling Mountains of Shaanxi province, China. Our field station (1800 m in altitude) lies on Sanguanmiao protection station (populated with more than 20 wild giant pandas), which is the core area of FNNR covering approximately 60 km² of habitat (1, 2). Given that the locations of horse fecal deposition are relatively fixed along the roads (set as transects, see also in *SI Appendix Fig. S2B*), 24 h-operated infrared camera-traps (Reconyx Hyperfire HC600, USA.) were mounted on trees by the roadside (40-60 cm in height) and used to record the HMR events. The camera-traps were programmed to capture 10 photos, with a delay of 0.1 s between each photo burst, and no quiet period before the next trigger. The time of captured images and ambient temperatures were simultaneously recorded. It was a happy accident that an HMR behavior exhibited by "Xiyue" (the name of this giant panda means happiness in Chinese, see also in *SI Appendix Movie S1*) was recorded (on New Year's Day in 2014) by Dr. Wenliang Zhou using a handheld camera. Meteorological data were obtained from the Foping Meteorological Station (E: 107° 58' 48", N: 33° 31' 12", 827.2 m in altitude). Given the altitude difference between the research base and the meteorological station, as shown in *Fig. 2C*, the temperature information was subtracted by 6 °C to represent the ambient temperatures of our field research base.

Volatiles analysis

To keep the stable property of chemicals, ten independent samples of horse manure (five fresh and five aged samples) were collected and stored at -80 °C. The supernatant of these samples was further analyzed using Gas Chromatography-Mass Spectrometry (GC-MS) following the manufacturer's protocol. Briefly, an Agilent Technologies Network 6890N gas chromatography system equipped with a 30m HP5-MS glass capillary column (0.25 mm i.d. × 0.25 μm film thickness) coupled with 5973 Mass Selective Detector was used to analyze volatiles. Thirty volatile chemical compounds were tentatively identified (see also in *SI Appendix Table S1*) by matching their retention time and mass spectra with structures available in the NIST 2002 library. All of these compounds were matched with an MS NIST spectral library (90% or higher). We converted the peak area of a particular compound (such as BCP or BCPO) into a percentage of the summed peak areas from the all GC peaks as a measure of the relative abundance of the relevant compound.

Mimicked dunghill

The hay (*Zoysia tenuifolia*) was shaped to mimic the dunghill of horses. The method for grouping these hays is indicated in *Fig. 2D*. All chemical compounds dissolved in pure water following the chemical composition are shown in *Appendix Table S3* were carefully sprayed over the grouped hays. The distance of adjacent hays was set as 3 m to minimize the mixing of volatiles. The visiting number and time spent on each access event by captive giant pandas in Beijing Zoo were recorded. Individual information of giant pandas is shown in *SI Appendix Table S2*. The HMR-like behavior of Ginny shown in *SI Appendix Movie S2* was recorded by Dr. Wenliang Zhou using a handheld camera.

Animals model and behaviors testing

Adult C57BL/6J mice (male, 23-25 g) were used for temperature preference testing (3). Mice were confined in an interconnected Plexiglas chamber on a metal surface, which contains two temperature plates set at 10 °C (cold plate) and 28 °C (warm plate), respectively. BCP/BCPO dissolved in pure water (100 μM) were carefully applied to four paws of each mouse (BCP/BCPO-treated mice, n=30). Saline was used in control group (saline-treated mice, n=30). The camera was used to record the behaviors of temperature preference for 5 minutes. The time spent by each mouse on the cold plate or warm plate was recorded. Especially, the number of crossing or retracting behavior was counted when the mice tried to move to the cold plate from the warm plate.

The cold-induced behaviors of mice were recorded by two cameras (for bright or infrared field, respectively). BCP/BCPO dissolved in pure water (100 μM) or saline were carefully applied to over the whole body of the mouse. Five BCP/BCPO-treated groups and five saline-treated groups were tested. Every five individuals were together kept in a clean cage at 4 °C for 24-hours video recordings.

Adult C57BL/6J mice (male, 23-25 g) were dosed with the mixture of icilin & saline (10 mg/kg i.p.) (n=8) and icilin & BCPO (100 umol/kg i.p.) (n=8), and adult wistar rats (male, 250-450 g) were dosed with the mixture of icilin & saline (1 mg/kg i.p.) (n=10) and icilin & BCPO (100 umol/kg i.p.) (n=10). Both of the mice and rats were placed individually in conical flasks, and monitored for spontaneous jumping and shakes behaviors over 10 min following injection. The data are expressed both as the group average number of jumps or shakes per minute.

Molecular biology

The cDNA sequences of gpTRMP8 and other tested receptors of giant panda were synthesized by Tsingke (Beijing, China) according to the predicted protein-encoding genes (XP_011221623 for cDNA of gpTRPM8) from the wild giant panda (*Ailuropoda melanoleuca*) genome (ACTA00000000.1). All cDNAs were subcloned into the pEGFPN1 vector as previously described (4). As previously reported (5), fluorescence protein eGFP was fused in frame to the C-terminus of gpTRPM8. The fusion of this fluorescence protein for determining the channel expression did not change channel function.

Transient transfection and electrophysiology

HEK 293 cells were cultured in Dulbecco's modified Eagle's medium (DMEM) with 10% fetal bovine serum, 1% penicillin/streptomycin and incubated at 37 °C in 5% CO₂. Cultured HEK-293 cells were transiently transfected with tested plasmid using Lipofectamine 3000 (Invitrogen), as described in a previous report (6). The function of expressed ion channels was identified by voltage-evoked or ligand-induced channel activation. Whole-cell configuration was used to record the cold- and menthol-induced currents of gpTRPM8.

All patch-clamp recordings were performed using a HEKA EPC10 amplifier with the PatchMaster software. Patch pipettes were prepared from borosilicate glass and fire-polished to a resistance of ~4 MΩ. Whole-cell recordings were used to test the BCP/BCPO sensitivity of each ion channel. For whole-cell recording, serial resistance was compensated by 60%. The current was sampled at 10 kHz and filtered at 2.9 kHz. Agonists and antagonists were perfused to a membrane patch by a gravity-driven system (RSC-200, Bio-Logic, 500 ms for solution switch). An independent solution was perfused through a separated tube to minimize the mixing of solutions. Patched cell or cell membrane was placed next to the perfusion tube outlet.

For TRPM8 recording, both pipette solution and bath solution contained (in mM): 130 NaCl, 3 HEPES, and 0.2 EDTA, pH was adjusted to 7.4 with NaOH.

For potassium channels, pipette solution contained (in mM): 120 KF, 20 NMG (N-methyl-D-glucamine), 10 HEPES, 11 EGTA, 2 MgATP, 0.5 Li₂GTP, pH was adjusted to 7.4 with KOH. The bath solution contained: 130 choline chloride, 5 KOH, 10 HEPES, 12 glucose, 2 MgCl₂, 2 CaCl₂, pH was adjusted to 7.4 with KOH.

For sodium channels, pipette solution contained (in mM): 20 NaCl, 135 CsF, 1 MgCl₂, 5 EGTA, 10 Glucose, and 10 HEPES, pH was adjusted to 7.4 with CsOH. The bath solution contained (in mM): 130 NaCl, 5 CsCl, 20 TEA-Cl, 1.8 CaCl₂, 5 4-AP, 0.01 verapamil-HCl, 0.1 NiCl₂, 1 CdCl₂, and 10 HEPES, pH was adjusted to 7.4 with NaOH (7).

Temperature control

Cold-induced channel activation was achieved by perfusion of precooled solutions. Solutions were cooled by embedding the solution reservoirs in ice cubes and then perfused through a separate line. The pipette was placed about 1 mm from the tube outlet. A TA-29 miniature bead thermistor (Harvard Apparatus) was used to ensure accurate monitoring of local temperature. Such temperature monitor was placed right next to the patched cell or cell membrane. The thermistor's temperature readout was fed into an analog input of the patch amplifier and recorded simultaneously with the whole-cell currents.

gpTRPM8 modelling

The partially modeled gpTRPM8 was constructed using the Rosetta molecular modeling suite version 2016.20 (8). The cryo-microscopy structure of TRPM8 in calcium-bound state (PDB: 6O77) was used as the template (9). Briefly, each round generated 10000 models. Among these models, the top 10 lowest-energy models were selected as the inputs for next round of loop modeling. After several rounds of KIC loop modeling, the top ten models converged well. The lowest-energy model was finally selected as the predicted structure of gpTRPM8 protein complex.

Data analysis

Phylogenetic analysis of protein sequences was carried out using MEGA version 6 (10). Data from electrophysiological recordings were analyzed using Igor Pro (WaveMatrix) and Prism (GraphPad). R 3.5.2 was used to analyze the data from animal assays (11). Pearson correlation was used to calculate the correlation coefficient (r). The data points are given as average \pm SEMs. The visit frequency and duration of captive pandas to different mimicked dunghill were compared by Kruskal-Wallis rank sum test. The R packages “dunn.test” for Kruskal–Wallis rank sum test were employed. Chi-square test was used to analyze the correlation between the freshness of horse manure with the HMR events. Wilcoxon rank sum test was used to test the difference between the two groups. We ran the Wilcoxon rank sum test using the “wilcox.test” function. Statistical significance was accepted at a level of $p < 0.05$. IC_{50} values were calculated from fitting a Hill equation to the BCPO/BCPO-induced concentration-response curve.

$$\frac{I_x}{I_{max}} = 1 - \frac{[X]^n}{IC_{50}^n + [X]^n}$$

Where I_x represents the difference between the BCPO/BCPO inhibited current in the presence of concentration $[x]$ and the current in the presence of saturated menthol, I_{max} represents the difference between the maximal current amplitude and the leaking current. IC_{50} is the concentration for the half-maximal effect.

To determine the threshold temperature, a linear fit was done for two phases (closed phase and activated phase). The intersect point of the two fitting lines was defined as the activation threshold temperature.

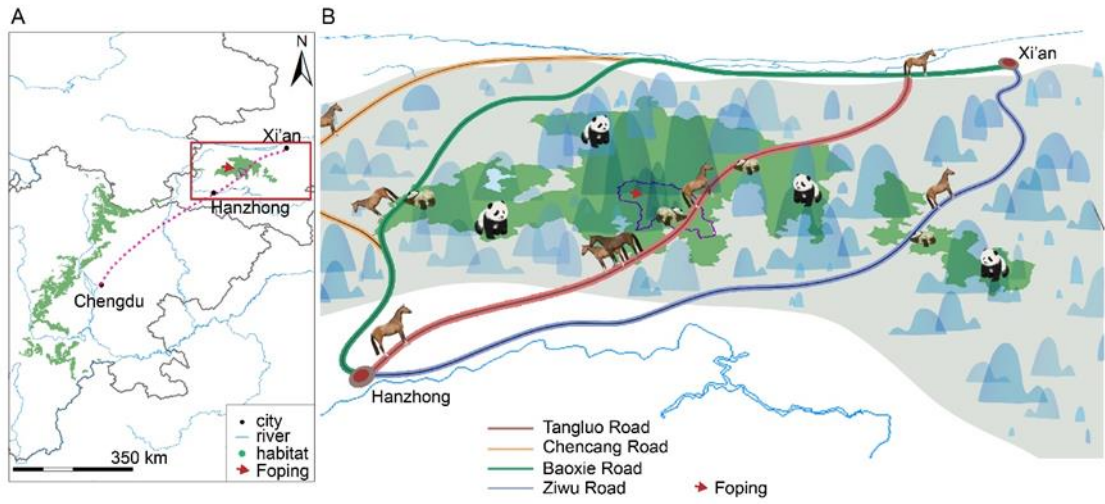


Fig. S1. Ancient trade routes (A) and possible panda-horse interactions (B).

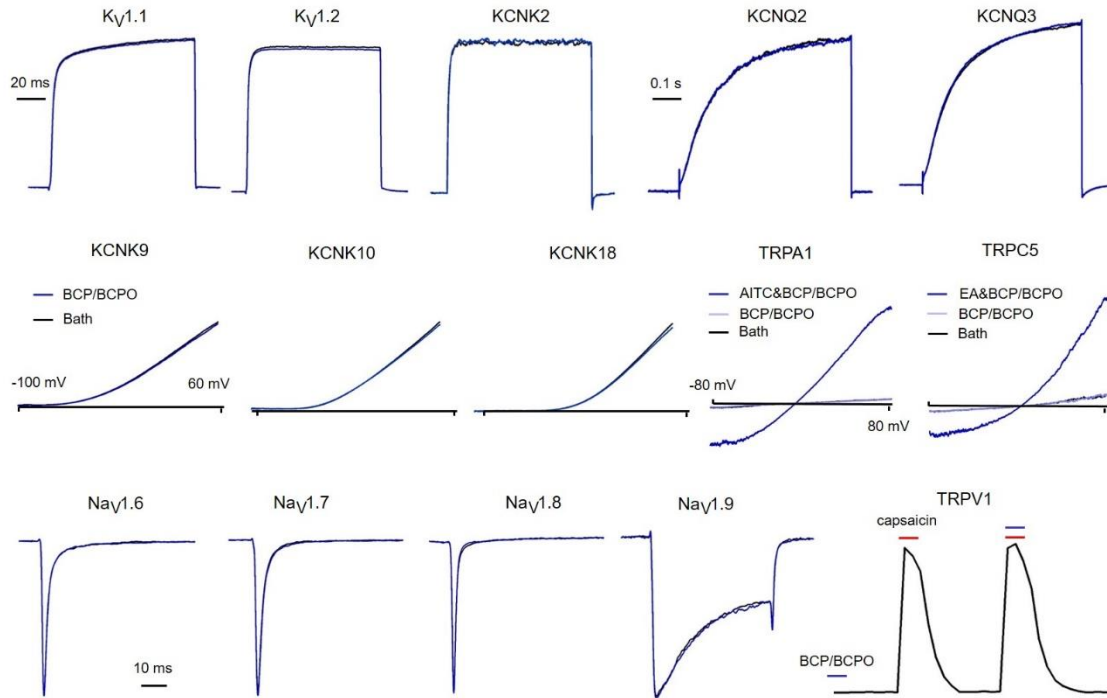


Fig. S2. Representative whole-cell currents of temperature-sensitive ion channels of giant panda in the presence of bath solution (black) and 10 μ M BCP/BCPO-containing bath solution (blue). Currents of $K_v1.1$ and $K_v1.2$ were elicited by a depolarization of 10 mV from a holding potential of -80 mV; to evoke KCNQ currents, a holding potential of -80 mV was used, from which a testing pulse to 0 mV was applied; whole cell currents of KCNK2 were evoked by a depolarization to 60 mV from a holding potential of -100 mV, and whole-cell recordings of KCNK9, KCNK10 and KCNK18 were subjected to a voltage ramp from -100 mV to 60 mV; TRPA1 and TRPC5 were subjected to a voltage ramp from -80 mV to 80 mV, for TRPV1 channel a holding potential of 0 mV was used from which a testing pulse to 80 mV was applied; for sodium channel subtypes ($Na_v1.6$, $Na_v1.7$, $Na_v1.8$ and $Na_v1.9$, current traces were evoked by a depolarization to -10 mV from a holding potential of -80 mV.

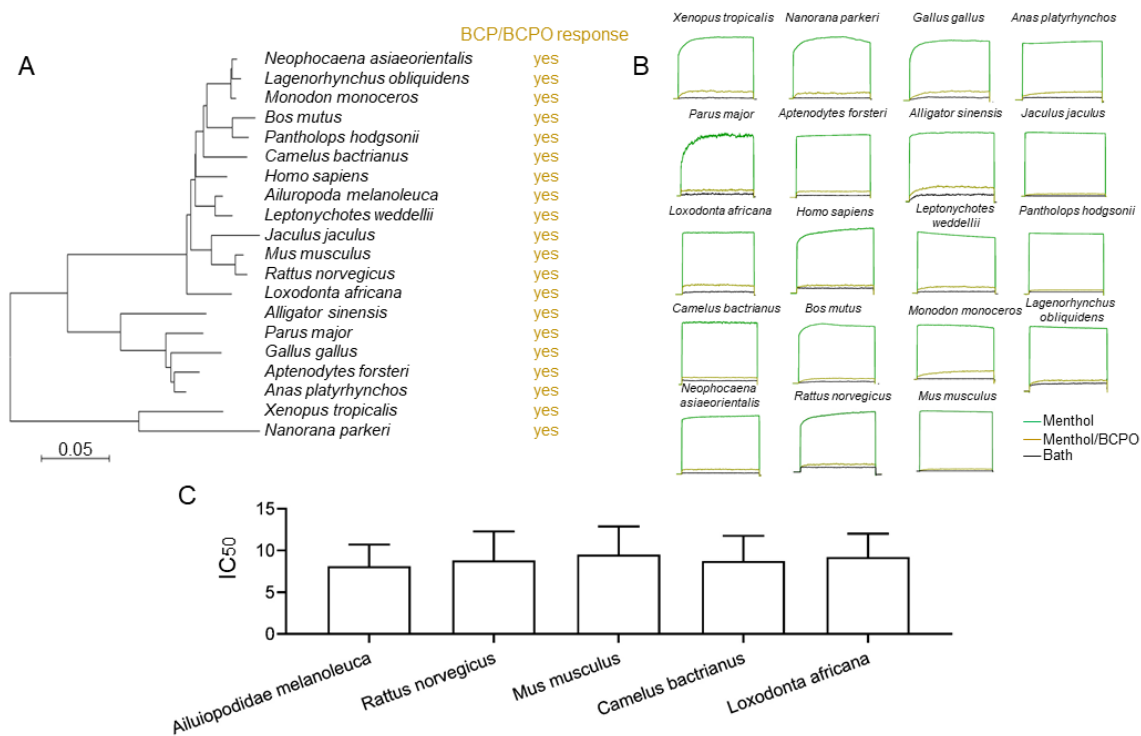


Fig. S3. (A) The antagonistic activity of BCP/BCPO on species-specific TRPM8 orthologs. Phylogenetic tree of these TRPM8 orthologs is shown. (B) Representative whole-cell recordings of 19 species-specific TRPM8 orthologs in the absence or presence of 10 μ M BCP/BCPO. TRPM8 currents were elicited by 80 mV from a holding potential of 0 mV. (C) The IC₅₀ of BCPO inhibition for cold-induced activation of TRPM8 orthologs. The cold-induced currents were recorded at -80 mV.

Table S1. Comparison of tentatively identified chemical composition of fresh and aged horse manure samples. The percentage (%) of each chemical compound showing the relative abundance in total volatiles.

Peak Number	Retention time (min)	Tentatively identified compounds	Molecular weight	Molecular formula	Fresh sample (%) (n=5)	Aged sample (%) (n=5)	P-value
1	4.86	Benzeneacetaldehyde	120	C8H8O	0.984±0.055	1.214±0.442	0.753
2	5.34	Phenol, 3-methyl- (<i>m</i> -Cresol)	108	C7H8O	0.705±0.041	1.206±0.433	0.139
3	7.8	Phenol, 4-(2-propenyl)-	134	C9H10O	3.561±0.693	1.060±0.050	0.265
4	8.4	Indole	117	C8H7N	0.537±0.056	0.564±0.212	0.691
5	9.63	1H-Indole, 3-methyl-	131	C9H9N	1.593±0.601	0.348±0.154	0.028
6	10.13	BCP	204	C15H24	3.573±0.424	0.471±0.086	0.007
7	10.55	. <i>alpha</i> -Caryophyllene	204	C15H24	0.887±0.122	0.151±0.000	0.010
8	10.79	2H-Indol-2-one, 1,3-dihydro-	133	C8H7NO	0.648±0.135	0.804±0.127	0.841
9	11.49	Phenol, 2,4-bis(1,1-dimethylethyl)-	206	C14H22O	0.916±0.146	0.405±0.033	0.095
10	12.14	BCPO	220	C15H24O	3.335±0.374	0.506±0.074	0.008
11	13.27	Tetradecanoic acid (branched)	228	C14H28O2	1.269±0.135	0.860±0.067	0.056
12	13.87	Tetradecanoic acid	228	C14H28O2	1.968±0.418	0.324±0.200	0.067
13	14.05	Pentadecanoic acid (branched)	242	C15H30O2	1.207±0.679	0.482±0.047	0.205
14	14.33	Octadecane	254	C18H38	1.202±0.141	0.622±0.067	0.420
15	14.82	Pentadecanoic acid	242	C15H30O2	3.248±0.309	2.585±0.218	0.421
16	15.36	Hexadecanoic acid	256	C16H32O2	1.449±0.431	3.027±0.234	0.059
17	16.34	Eicosane	282	C20H42	0.756±0.101	0.481±0.045	0.834
18	17.14	1-Hexadecanol, 3,7,11,15-tetramethyl-	298	C20H42O	8.241±0.615	4.203±0.535	0.008
19	17.28	Heneicosane	296	C21H44	1.670±0.174	0.796±0.085	0.834
20	17.46	Phytol	296	C20H40O	5.989±1.013	2.748±0.605	0.032
21	18.17	Docosane	310	C22H46	0.940±0.123	0.464±0.049	0.548
22	19.03	Tricosane	324	C23H48	1.453±0.263	0.859±0.119	0.222
23	19.86	Tetracosane	338	C24H50	1.061±0.153	1.299±0.234	0.421
24	20.65	Pentacosane	352	C25H52	1.776±0.160	2.055±0.235	0.691
25	21.41	Hexacosane	366	C26H54	2.075±0.069	2.568±0.130	0.032
26	22.15	Heptacosane	380	C27H56	3.087±0.474	3.756±0.561	0.421
27	22.95	Octacosane	394	C28H58	1.919±0.232	2.963±0.165	0.055
28	23.3	1,19-Eicosadiene	278	C20H38	2.507±0.254	3.107±0.263	0.151
29	23.88	1-Docosene	308	C22H44	3.237±0.386	4.254±0.715	0.222
30	24.14	Cholesta-3,5-diene	368	C27H44	19.545±2.606	14.374±1.054	0.841

Table S2. Individual information of giant pandas in Beijing Zoo.

Individual	Age	Sex	Weight (kg)
Dadi	25	Male	115
Gugu	21	Male	110
Ginny	24	Female	90
Mengda	6	Male	107
Menger	6	Male	108
Fulu	7	Female	101

Table S3. Chemical compounds used for mimicking dunghills.

VOC	Functional Group	Group A	Group B	Control C
BCP	Sesquiterpene	1ml/L	0	0
BCPO	Sesquiterpene	1g/L	0	0
Tetradecanoic acid	Hydrocarbon acid	0	1g/L	0
Pentadecanoic acid	Hydrocarbon acid	0	1g/L	0
Hexadecanoic acid	Hydrocarbon acid	0	1g/L	0

Movie S1. Representative HMR behaviors recorded by handheld (up) and infrared (bottom) cameras in the field.

Movie S2. BCP/BCPO-induced HMR-like behavior of Ginny.

Movie S3. Temperature preference testing on saline-treated and BCP/BCPO-treated mice.

Movie S4. Cold-induced behaviors of saline-treated and BCP/BCPO-treated mice at 4 °C.

SI References

1. Hu YB, *et al.* (2017) Inbreeding and inbreeding avoidance in wild giant pandas. *Mol Ecol* 26(20):5793-5806.
2. Wei W, *et al.* (2015) Hunting bamboo: Foraging patch selection and utilization by giant pandas and implications for conservation. *Biol Conserv* 186:260-267.
3. Luo L, *et al.* (2019) Molecular basis for heat desensitization of TRPV1 ion channels. *Nature communications* 10(1):2134.
4. Han Y, *et al.* (2018) Molecular mechanism of the tree shrew's insensitivity to spiciness. *PLoS biology* 16(7):e2004921.
5. Yang S, *et al.* (2017) A bimodal activation mechanism underlies scorpion toxin-induced pain. *Science advances* 3(8):e1700810.
6. Yang S, *et al.* (2015) A pain-inducing centipede toxin targets the heat activation machinery of nociceptor TRPV1. *Nat Commun* 6:8297.
7. Li B, *et al.* (2019) Molecular game theory for a toxin-dominant food chain model, *Natl Sci Rev*, 6(6): 1191-1200.
8. Leaver-Fay A, *et al.* (2011) ROSETTA3: an object-oriented software suite for the simulation and design of macromolecules. *Methods Enzymol* 487:545-574.
9. Diver MM, Cheng YF, & Julius D (2019) Structural insights into TRPM8 inhibition and desensitization. *Science* 365(6460):1434-+.
10. Kumar S, Stecher G, Li M, Knyaz C, & Tamura K (2018) MEGA X: Molecular Evolutionary Genetics Analysis across Computing Platforms. *Mol Biol Evol* 35(6):1547-1549.
11. R Core Team (2013) R: A language and environment for statistical computing.